

On the handedness of helical aggregates of C_3 tricarboxamides. A multichiroptical characterization

Belén Nieto-Ortega,^a Fátima García,^b Giovanna Longhi,^c Ettore Castiglioni,^c Joaquín Calbo,^d
Sergio Abbate,^c Juan T. López Navarrete,^{*a} Francisco J. Ramírez,^a Enrique Ortí,^{*d} Luis
Sánchez^{*b} and Juan Casado^{*a}

^a *Departamento de Química Física. Facultad de Ciencias. Universidad de Málaga, Campus de Teatinos s/n, 29071 Málaga (Spain). Fax: (+) 34952132000; E-mail casado@uma.es.*

^b *Departamento de Química Orgánica, Facultad de Ciencias Químicas, Ciudad Universitaria s/n. 28040 Madrid (Spain), Fax: (+) 34913944103; E-mail: lusamar@quim.ucm.es.*

^c *Dipartimento di Medicina Molecolare e Traslazionale, Università di Brescia, 25123 Brescia, (Italy). Fax: (+) 390303701157; E-mail: sergio.abbate@unibs.it.*

^d *Instituto de Ciencia Molecular, Universidad de Valencia, 46980 Paterna (Spain); E-mail: enrique.orti@uv.es.*

Contents:

<i>1.- Supplementary Figures</i>	<i>S-2</i>
<i>ECD spectra of (S)-1 in mixtures MCH/CHCl₃</i>	<i>S-2</i>
<i>Calculated ECD and UV-Vis spectra</i>	<i>S-2</i>
<i>Fluorescence spectra of (S)-1 increasing the time</i>	<i>S-3</i>
<i>Calculated emission spectrum of 1</i>	<i>S-4</i>
<i>CPL measurments</i>	<i>S-4</i>
<i>2.- CPL test on (R)-1</i>	<i>S-7</i>
<i>3.- Theoretical calculations</i>	<i>S-8</i>
<i>4.- Experimental section</i>	<i>S-10</i>
<i>X.- References</i>	<i>S-11</i>

1. Supplementary Figures

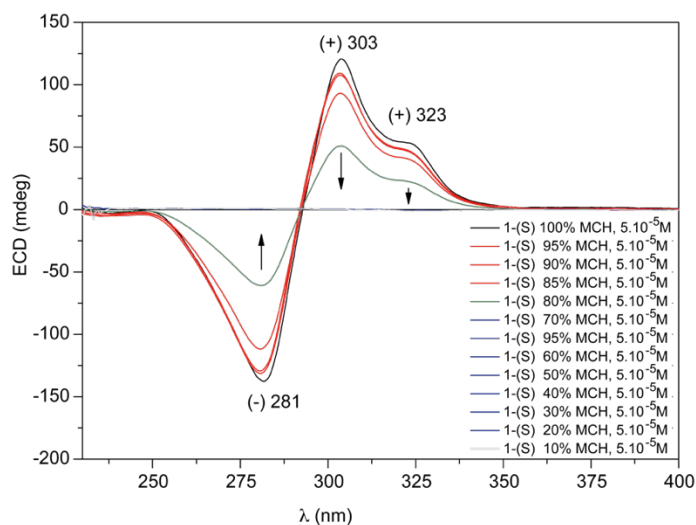


Figure S1. ECD spectra of tricarboxamide (*S*)-**1** in different MCH/CHCl₃ mixtures, ranging from the two pure solvents, at a fixed concentration of 5×10^{-5} M at 298 K.

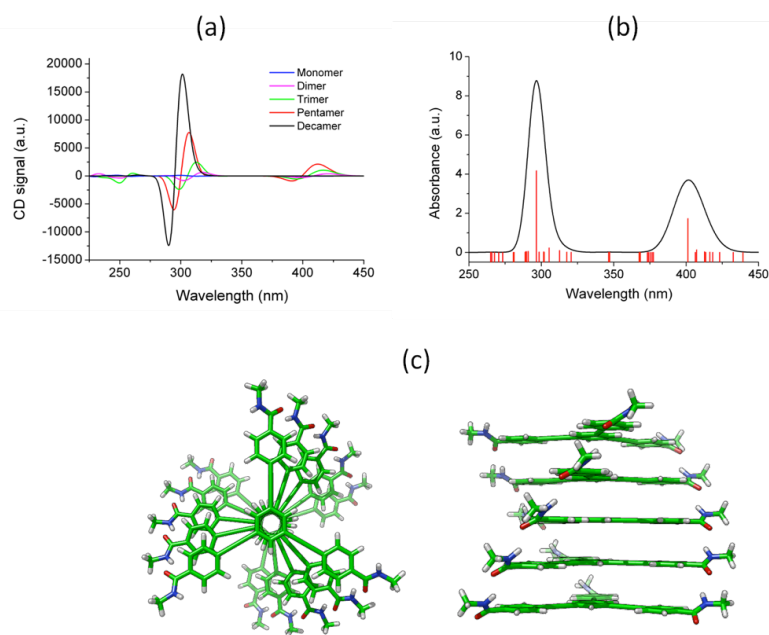


Figure S2. (a) Theoretical simulation of the ECD spectrum computed at the PM6/CIS level for right-handed aggregates from one to ten monomeric units. For the decamer, the calculated wavelength window covers the 345–265 nm region. (b) UV-Vis spectrum computed for the pentamer. Vertical red lines represent the value of the oscillator strength (f) for each excited state calculated. (c) Top (left) and side (right) view of the right-handed pentamer showing the triple array of H-bonds forming the helical structure.

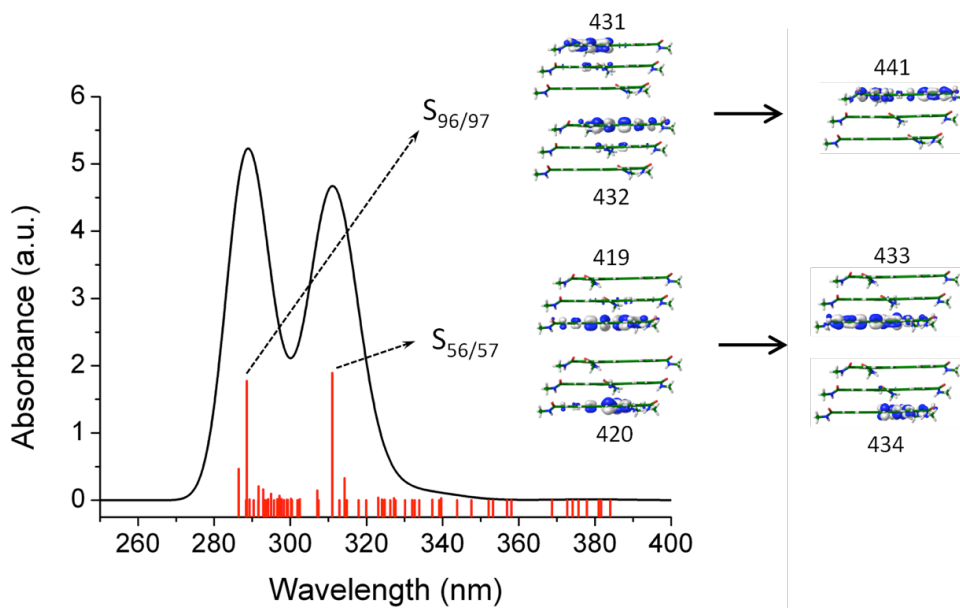


Figure S3. TD-DFT UV-Vis spectrum for the right-handed trimer computed at the TDA-B3LYP/6-31G* level for the lowest-lying 100 singlet excited states. Vertical red lines represent the value of the oscillator strength (f) for each excited state calculated. The main one-electron excitations participating in the $S_0 \rightarrow S_{56/57}$ and $S_0 \rightarrow S_{96/97}$ transitions are shown.

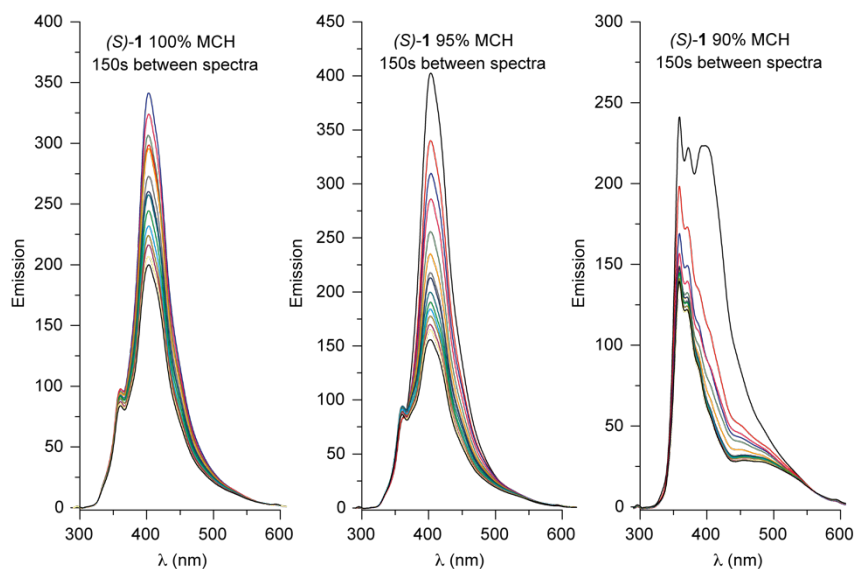


Figure S4. Time fluorescence spectra of tricarboxamide (**(S)-1**) in different MCH:CHCl₃ mixtures at a fixed concentration of 5×10^{-5} M at 298 K.

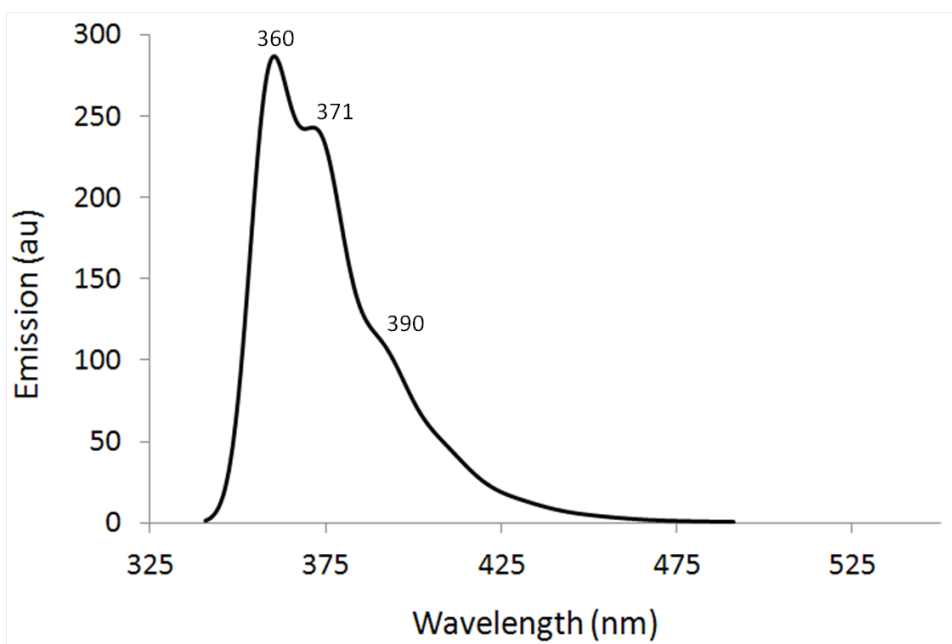


Figure S5. Vibrationally-resolved electronic spectrum calculated at the TD-B3LYP/6-31G** level of theory for the $S_1 \rightarrow S_0$ emission of the monomer of **1**. The calculated spectrum was shifted in the wavelength axis to match the most intense peak experimentally recorded at 360 nm.

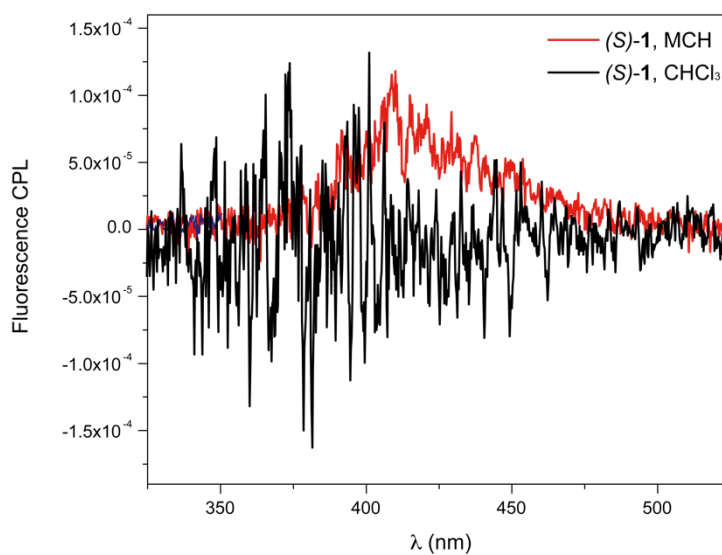


Figure S6. CPL spectra of (*S*)-**1** in MCH and CHCl_3 (5×10^{-5} M, $\lambda_{\text{exc}} = 297$ nm, at 298 K).

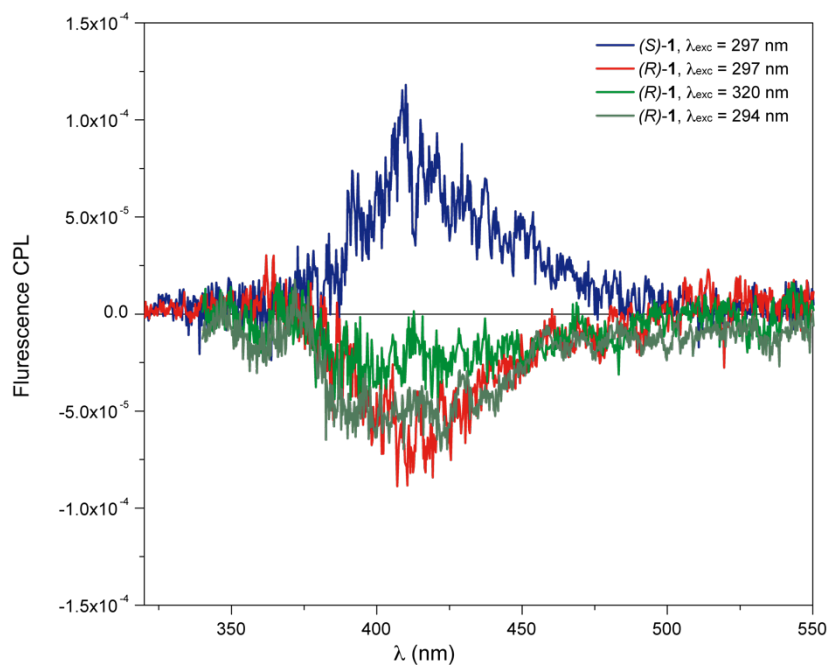
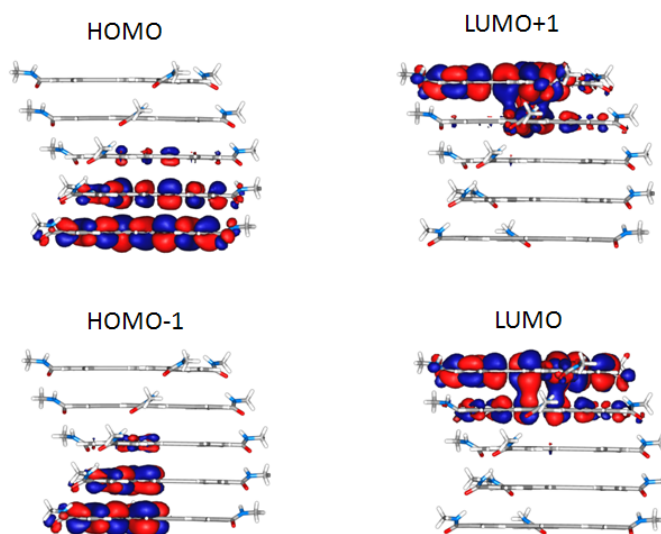


Figure S7. CPL spectra of (*S*)-1 and (*R*)-1 at different λ_{exc} (MCH, 5×10^{-5} M, at 298 K).

Table S1. Lowest-energy singlet excited states calculated for the right-handed pentamer of tricarboxamide **1** at the TDA-B3LYP/6-31G* level. Vertical excitation energies (E), oscillator strengths (f) and dominant monoexcitations with contributions (within parentheses) greater than 20% are summarized. Molecular orbitals involved in the lowest electronic transitions are depicted in the adjacent figure.

State	E (eV)	E (nm)	f	Monoexcitation ^a
S1	2.641	469.5	0.000	H-1 \rightarrow L (28)
				H-1 \rightarrow L+1 (20)
				H \rightarrow L (21)
				H \rightarrow L+1 (29)
S2	2.645	468.8	0.000	H-1 \rightarrow L+1 (49)
				H \rightarrow L (49)
S3	2.645	468.8	0.000	H-1 \rightarrow L (49)
				H \rightarrow L+1 (49)
S4	2.649	468.1	0.000	H-1 \rightarrow L (21)
				H-1 \rightarrow L+1 (29)
				H \rightarrow L (28)
				H-1 \rightarrow L (20)

^a H and L denote HOMO and LUMO, respectively.



2. CPL test

In order to check the chiral response, the CPL spectrum of **(R)-1** was recorded in MCH solution at $\approx 10^{-5}$ M concentrate. Since aggregation does not take place, the CPL results silent. The CPL spectrum of **(R)-1** was also recorded by using excitation wavelengths of 320 nm (shoulder observed on the high wavelength side in the CD spectrum), and 294 nm, the point where the ECD spectrum is zero (Fig. S7). In the latter case, no correction for the differential right and left circularly polarized absorption of the excitation beam is needed. These two last experiments depict the same shape of the CPL spectrum (a little less intense in the case of 320 nm) than that shown in Fig. 3 in the main text.

3. Theoretical calculations

Preliminary evaluation of the electronic circular dichroism (ECD) spectrum was carried out at the PM6-CIS level. The semiempirical PM6^[1] hamiltonian was combined with configuration interaction using single-excitation (CIS)^[2] calculations for the 100 lowest-lying singlet excited states. Oligomers with $n = 1, 2, 3, 5$ and 10 units were modeled in a right-handed fashion, and the calculated ECD spectra are shown in Fig. S2a. For the decamer, the PM6-CIS calculation was performed for the 100 singlet excited states with energies greater than 3.60 eV ($\lambda \leq 345$ nm). To significantly alleviate the computational effort, the long aliphatic chains of **1** were substituted in all cases by short methyl groups since they do not participate in the electronic features of the supramolecular assembly. The intermolecular parameters to generate the stacking were extracted after a fully optimization of a right-handed pentamer as previously (intermolecular distance of 3.275 Å and rotation of 18.0° along the growing axis).^[3] The corresponding UV-Vis spectrum for the pentamer at the PM6-CIS level is depicted in Fig. S2b. The most intense electronic transition is computed at 300 nm as a doubly degenerate singlet state $S_{57/58}$, which gives rise to the $-/+$ intense band that appears around 300 nm in the theoretical ECD spectrum calculated for the right-handed oligomers of tricarboxamide **1** (Fig. S2a).

More accurate calculations at the time-dependent density functional theory (TD-DFT)^[4] level were performed in a second step for the aggregate including three OPE-TA. The Tamm-Dancoff approach (TDA)^[5] was used to save computational resources. Fig. S3 displays the theoretical UV-Vis spectrum calculated for the right-handed trimer under the TDA approach with the B3LYP functional^[6] and the 6-31G* basis set^[7] for the 100 lowest-lying singlet excited states. The most intense transitions correspond to doubly-degenerate singlet states $S_{56/57}$ and $S_{96/97}$ with oscillator strengths of 1.89 and 1.77, respectively. Although these states have a large configurational character, they mainly originate from electron monoexcitations between the orbitals located on the edges of the supramolecular aggregate (Fig. S3). The theoretical ECD calculated at this level of theory is shown in Fig. 1c in the main text, where the electronic

transitions (vertical lines) giving shape to the spectrum are depicted. The $-/+$ pattern computed for the right-handed trimer unequivocally matches the experimental ECD spectrum recorded for **(S)**-**1**. Likewise, the left-handed trimer exhibits a mirror-like ECD spectrum and is assigned to the enantiomer **(R)**-**1**.

TD-DFT calculations were carried out to simulate the emission spectrum of **1**. Figure S5 shows the convoluted vibrationally-resolved electronic spectrum calculated for the emission from the first singlet excited state (S_1) to the ground state (S_0) of **1** as a monomer at the TD-B3LYP/6-31G** level. The electronic transition dipole moment was developed in a Taylor series about the equilibrium geometry of the final state up to the first-order term included according to the Franck-Condon-Herzberg-Teller approach.^[8] The half-width at half-maximum of the Gaussian functions used to convolute the spectrum was set at 250 cm^{-1} . The calculated spectrum was shifted in the wavelength-axis to match the most intense peak experimentally recorded at 360 nm.

TD-DFT calculations were also performed for the right-handed pentamer aggregate of **1** to shed light on the nature of the lowest-lying singlet excited states for the supramolecular stack. The 4 lowest-energy electronic transitions correspond to multiconfigurational excitations with no oscillator strength and with a large delocalization along the supramolecular entity (Table S1). All these transitions are mainly described by one-electron promotions from the HOMO and HOMO-1, which are located in one end of the oligomer, to the LUMO and LUMO+1, mainly distributed in the other end.

All the calculations were carried out by means of the Gaussian 09 (version D.01)^[9] suite of programs. Molecular orbitals were plotted using Chemcraft 1.6.^[10]

4. Experimental section

Materials. The preparation of the tricarboxamides (**S**)-**1** and (**R**)-**1** requires only three synthetic steps from commercial reagents, and their completely synthesis were published in elsewhere (Ref. 5a in the main text).

Electronic spectroscopy. Electronic circular dichroism (ECD) spectra were recorded using a Jasco © 815SE. The experimental settings were: 25 °C, scan rate of 200 nm min⁻¹ of scan speed, spectral resolution of 1nm and 2.0 mm path-length quartz cell. Solutions at a standard concentration of 5×10^{-5} M were prepared using methylcyclohexane (MCH) and CHCl₃ as solvents. The spectrometer was continuously purged with dry N₂ gas. Home-made equipment, interfaced with a Jasco FP8200 fluorimeter, was used for CPL measurements, as previously described.^[11] The CPL experimental settings were: beam collection at 90° respect to the excitation radiation, with a fluorescence quartz cell 2 mm-long in the excitation side and 10 mm in the emission side, 30 nm min⁻¹ of scan rate, 2 seconds of integration time and 10 accumulated scans for each spectrum.

Vibrational spectroscopy. Vibrational Circular Dichroism (VCD) spectra were recorded in a PMA50 optical bench coupled to a Vertex70 spectrometer, both supplied by Bruker ©. In the PMA50, the infrared radiation (3800-600 cm⁻¹ range) is focused by a BaF₂ lens toward a ZnSe photo-elastic modulator (PEM, 50 kHz frequency). The circularly polarized beam is then driven to the sample and finally collected by a D313/QMTC detector. To ensure a proper chiroptical signal within a spectral region of 600 cm⁻¹ around the tuning wavenumber, a calibration of the PEM at a fixed wavenumber had been used before recording any VCD spectrum. Typically, calibrations at 1400 cm⁻¹ allowed us to obtain a spectrum over the most meaningful region for conjugated organic systems. Every VCD spectrum was the result of averaging a minimum of 8000 scans, equivalent to 6 h of acquisition time, recorded at a spectral resolution of 4 cm⁻¹. To

ensure the absence of linear dichroism interference, caused by preferential orientations within the gels,^[12] spectra on different aliquots of these compounds were recorded at different angles without observing appreciable deviations. As a proof of the quality of the recorded data, spectra from pure enantiomeric samples result in mirror images (see Fig. 2 in the main text). The samples (**S**)-**1** and (**R**)-**1** in MCH at 3×10^{-3} M concentration were prepared for vibrational spectra measurements. After thermal treatment, the samples were placed, at room temperature, in a demountable cell A145 (Bruker, Germany) supplied with KBr windows. At this concentration both enantiomers are in gel state. A 15 μm Teflon spacer was used to obtain the optimal IR signal for VCD.

References

- [1] J. J. P. Stewart, *J. Mol. Model.* 2007, **13**, 1173.
- [2] J. B. Foresman, M. Head-Gordon, J. A. Pople and M. J. Frisch, *J. Phys. Chem.* 1992, **96**, 135.
- [3] F. García, P. M. Viruela, E. Matesanz, E. Ortí and L. Sánchez, *Chem. Eur. J.* 2011, **17**, 7755.
- [4] a) M. E. Casida, C. Jamorski, K. C. Casida and D. R. Salahub, *J. Chem. Phys.* 1998, **108**, 4439; b) C. Jamorski, M. E. Casida and D. R. Salahub, *J. Chem. Phys.* 1996, **104**, 5134; c) M. Petersilka, U. J. Gossmann and E. K. U. Gross, *Phys. Rev. Lett.* 1996, **76**, 1212.
- [5] J. C. Taylor, *Physical Review* 1954, **95**, 1313.
- [6] a) C. Lee, W. Yang and R. G. Parr, *Phys. Rev. B* 1988, **37**, 785; b) A. D. Becke, *J. Chem. Phys.* 1993, **98**, 5648.
- [7] M. M. Francl, W. J. Pietro, W. J. Hehre, J. S. Binkley, M. S. Gordon, D. J. Defrees and J. A. Pople, *J. Chem. Phys.* 1982, **77**, 3654.
- [8] F. Santoro, A. Lami, R. Improta, J. Bloino and V. Barone, *J. Chem. Phys.* 2008, **128**, 224311.
- [9] Gaussian 09, Revision D.01, M. J. Frisch, G. W. Trucks, H. B. Schlegel, G. E. Scuseria, M. A. Robb, J. R. Cheeseman, G. Scalmani, V. Barone, B. Mennucci, G. A. Petersson, H. Nakatsuji, M. Caricato, X. Li, H. P. Hratchian, A. F. Izmaylov, J. Bloino, G. Zheng, J. L. Sonnenberg, M. Hada, M. Ehara, K. Toyota, R. Fukuda, J. Hasegawa, M. Ishida, T. Nakajima, Y. Honda, O. Kitao, H. Nakai, T. Vreven, J. A. Montgomery, J. E. Peralta, F. Ogliaro, M. Bearpark, J. J. Heyd, E. Brothers, K. N. Kudin, V. N. Staroverov, R. Kobayashi, J. Normand, K. Raghavachari, A. Rendell, J. C. Burant, S. S. Iyengar, J. Tomasi, M. Cossi, N. Rega, J. M. Millam, M. Klene, J. E. Knox, J. B. Cross, V. Bakken, C. Adamo, J. Jaramillo, R. Gomperts, R. E. Stratmann, O. Yazyev, A. J. Austin, R. Cammi, C. Pomelli, J. W. Ochterski, R. L. Martin, K. Morokuma, V. G. Zakrzewski, G. A. Voth, P. Salvador, J. J. Dannenberg, S. Dapprich, A. D. Daniels, Farkas, J. B. Foresman, J. V. Ortiz, J. Cioslowski and D. J. Fox, Gaussian, Inc., Wallingford CT, 2009.
- [10] ChemCraft 1.8, G. A. Zhurko,
- [11] E. Castiglioni, S. Abbate and G. Longhi, *Appl. Spectrosc.* 2010, **64**, 1416.
- [12] A. Brizard, D. Berthier, C. Aimé, T. Buffeteau, D. Cavagnat, L. Ducasse, I. Huc and R. Oda, *Chirality* 2009, **21**, E153.